Bound states in the continuum in anisotropic plasmonic metasurfaces

Yao Liang[1] ‡, Kirill Koshelev[2,3] ‡, Fengchun Zhang[4] ‡, Han Lin[1], Shirong Lin[1], Jiayang Wu[5], Baohua Jia[1] *, and Yuri Kivshar[2,3] *

[1]Centre of Translational Atomaterials (CTAM), Faculty of Science, Engineering and Technology, Swinburne University of Technology, Hawthorn, VIC 3122, Australia

[2]Nonlinear Physics Center, Research School of Physics, Australian National University, Canberra, ACT 2601, Australia

[3]Department of Physics and Engineering, ITMO University, St Petersburg 197101, Russia

[4]Institute of Semiconductor Science and Technology, South China Normal University, Guangzhou 510631, China

[5]Centre for Light Science, Faculty of Science, Engineering and Technology, Swinburne University of Technology, Hawthorn, VIC 3122, Australia

ABSTRACT

The concept of optical bound states in the continuum (BICs) currently drives the field of dielectric resonant nanophotonics, and it provides an important physical mechanism for engineering high-quality (high-Q) optical resonances in individual high-index dielectric nanoparticles and structured dielectric metasurfaces. For structured metallic metasurfaces, realization of BICs remains a challenge associated with strong dissipative losses of plasmonic materials. Here, we suggest and realize experimentally *anisotropic plasmonic metasurfaces* supporting high-Q resonances governed by quasi-BIC collective resonant modes. Our metasurfaces are composed of arrays of vertically oriented double-pillar meta-molecules with high aspect ratio covered by a thin layer of gold. We engineer quasi-BIC modes with highly anisotropic dispersion in the reciprocal space and observe experimentally sharp resonances in mid-IR reflectance spectra. Our work suggests a direct route to boost the resonant field enhancement in plamonic metasurfaces via combining a small effective mode volume of plasmonic systems with engineered high-Q resonances provided by the BIC physics, with multiple applications to enhance light-matter interaction for nano-optics and quantum photonics.

KEYWORDS

Plasmonic nanostructures offer strong subwavelength localisation of light,[1] with widespread applications that range from single-photon emitters and nanoscale imaging to ultrafast lasing and nonlinear optics.[2-4] Metal nanoparticle arrays that support surface lattice resonances have emerged as an exciting platform for manipulating light–matter interactions at the nanoscale and enabling a diverse range of applications.[5] In contrast to recently highlighted field of the Mie-resonant dielectric nanophotonics[6,7] where the field localization occurs mainly inside nanoparticles, the plasmonic systems such as arrays of metallic nanoparticles confine energy at the metal-dielectric interfaces with surface plasmonic resonances.[8] Surface plasmon resoanances are ultra-sensitive to a local change of the reflective index and provide strong near-field enhancement of light associated with their small mode volume.[1] However, the quality factor (Q-factor) of plasmon resonances is often limited due to intrinsic dissipative and radiative losses. [9] The plasmonic nanoparticle structures with high-Q resonances and suppressed losses would be beneficial for many applications that require sharp resonant response and strong enhancement of light-matter interaction.[10]

Recent developments of resonant dielectric structures with high-Q resonances have attracted a lot of attention to the physics of optical bound states in the continuum[11] (BICs) earlier studied mainly for photonic crystals and waveguide arrays.[12-14] BICs were introduced in quantum mechanics almost a hundred years ago, and only in the last decade their rich physics was applied to engineer sharp resonances in the form of quasi-BICs in a variety of photonic systems.[15] By now, optical BICs have been predicted and observed essentially in dielectric structures such as individual subwavelength nanoparticles[16] and metasurfaces[17], and used for various applications including lasing[18, 19], sensing[20] and nonlinear optics[21].

The explorations of BICs in plasmonic structures remain mainly excluded due to their intrinsic losses,[1] and experimental demonstrations of plasmonic BICs have been restricted to long

wavelengths, such as terahertz (THz) regime, where the Ohmic loss is small and metals can be studied as perfect electric conductors.[22, 23] At shorter wavelengths, such as mid-infrared (mid-IR) or visible ranges, noble metals (i.e., gold or silver) exhibit significant metallic losses and thus pose a challenge for the realization of BIC modes and the observation of associated resonant effects. Recently, the realization of BICs in hybrid plasmonic system at visible frequencies was predicted theoretically.[24] This was achieved by employing a combination of metallic gratings and dielectric slabs to eliminate radiation losses in metals.

Here, we demonstrate a plasmonic metasurface supporting quasi-BIC modes in the mid-IR frequency range manifested as sharp resonances in the reflection spectra. The engineered metasurface is composed of a periodic lattice of pairs of connected pillar resonators with high aspect ratio. We reveal that the radiative losses in such plasmonic arrays can be entirely eliminated by employing the physics of symmetry-protected BICs, and high Q factors limited only by the dissipation losses can be achieved. The anisotropy of double-pillar meta-molecules is employed to enable highly anisotropic dispersion of the quasi-BIC with the opposite group velocities along the principal axes of the reciprocal space. We fabricate a metasurface with the femtosecond laser writing technique via two-photon polymerization and cover it by a 100-nm layer of gold. Using Fourier transform infrared spectroscopy (FTIR), we observe sharp dips in the spectra associated with the plasmonic quasi-BIC. In experiment, we study quasi-BICs in the vicinity of the perfect absorption condition, for which the field enhancement is the highest. To enable selective excitation of the quasi-BICs beyond the limit of the standard FTIR, we introduce angle selectivity to the reflective objective which filters the angular dispersion of the incident beam. By demonstrating sharp resonances in the plasmonic metasurface, we have challenged one of the critical limitations of plasmonic nanostructures, for which strong field enhancement is associated traditionally with a

small mode volume rather than a high Q factor. Our demonstration opens up a new avenue for plasmonic metasurfaces as a platform for specific applications in light-matter interaction, nonlinear photonics, quantum optics, and spectroscopy.

RESULTS AND DISCUSSION

Our plasmonic metasurface consists of a photonresist-base layer covered with a 100-nm film of gold, which is patterned with a structured lattice of anisotropic subwavelength meta-molecules (see Figure 1a). The metal film is thick enough to prevent transmission at the mid-IR wavelengths. [25] Each meta-molecule consists of two vertical pillars with a high aspect ratio (~3) connected with a narrow bridge, with the geometrical parameters defined in Figure 1b. The parameters are P = 3.2 μm, H = 1.7 μm, h = 0.6 μm, L = 1.15 μm, w = 0.5 μm, D = 0.6 μm, and t = 0.1 μm. The use of a three-dimensional geometry enables an extra degree of freedom for control of mode properties. [26]
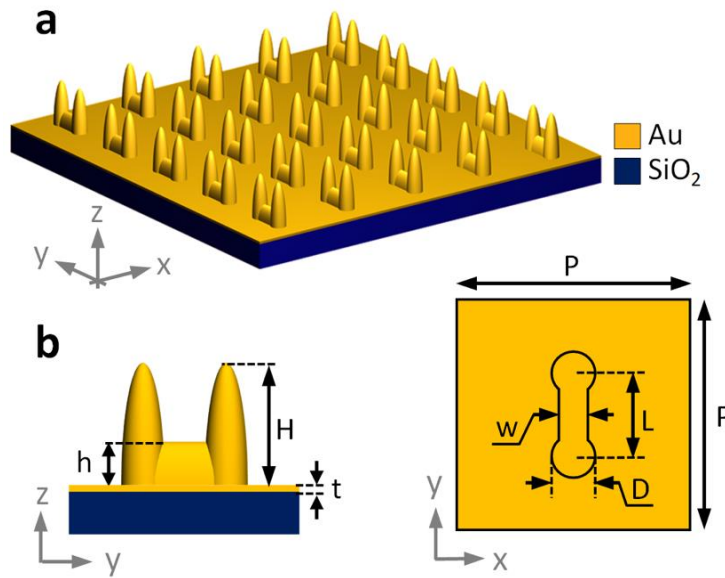

Figure 1. Plasmonic metasurface supporting quasi-BIC resonant modes. (a) Schematic of the array composed of a lattice of double pillars. (b) Side and top views of the unit cell.

The designed metasurface supports several BIC modes, protected by the in-plane inversion symmetry of the meta-molecule. [17] Ideal BICs with infinite Q factor only exist in lossless infinite structures or in structures with infinite or zero permittivity. [11] In lossy plasmonic structures, the total Q factor Q_{tot} is defined by the expression $Q_{tot}^{-1} = Q_{rad}^{-1} + Q_{dis}^{-1}$, where Q_{rad} and Q_{dis} are the radiative and dissipative quality factors, respectively. The dissipative losses responsible for material absorption transform BICs into quasi-BICs with a high yet finite Q_{tot}.

Below the diffraction limit, quasi-BICs radiate into a zeroth-order diffraction channel only, which determines the rate of Q_{rad}. With an increase of the angle of incidence, Q_{rad} drops drastically while Q_{dis} can be considered constant. At the resonance, the field enhancement $|E|^2/|E_0|^2$ can be expressed as[27]

$$\frac{|E|^2}{|E_0|^2} \propto \frac{Q_{tot}^2}{V_{eff}\, Q_{rad}}.$$
(1)

Here, E_0 is the amplitude of the incident field and V_{eff} is the effective mode volume. For plasmonic structures. V_{eff} is usually deeply subwavelength which guarantees a strong field enhancement at the resonance. Equation (1) shows that other two factors which govern the field enhancement are (i) the absolute value of the total Q factor Q_{tot} and (ii) the ratio of the radiative and dissipative Q factors Q_{rad}/Q_{dis}. To increase Q_{tot} and keep V_{eff} small, we focus on the fundamental (dipolar) BIC with both small effective mode volume and high Q factor. To engineer the ratio of radiative and dissipative losses, we change the angle of incidence, which affects the value of Q_{rad} dramatically. In the BIC regime (for normal incidence), $Q_{rad} \to \infty$ and $Q_{tot} = Q_{dis}$, while the field enhancement vanishes. For very large angles of incidence, $Q_{rad} \ll Q_{dis}$, and the field enhancement is also small being proportional to the radiative Q factor. Equation (1) shows that the highest field enhancement can be achieved for an intermediate regime, when $Q_{dis} = Q_{rad}$. This condition is known as the optimal (or, critical) coupling, and it is widely studied in applications to plasmonics, metamaterials, and other areas[28,29]. Importantly, for plasmonic structures this condition coincides

with the condition of perfect absorption (PA).[30] Therefore, to achieve the highest field enhancement, we need to study the quasi-BIC mode in the regime of the perfect absorption.
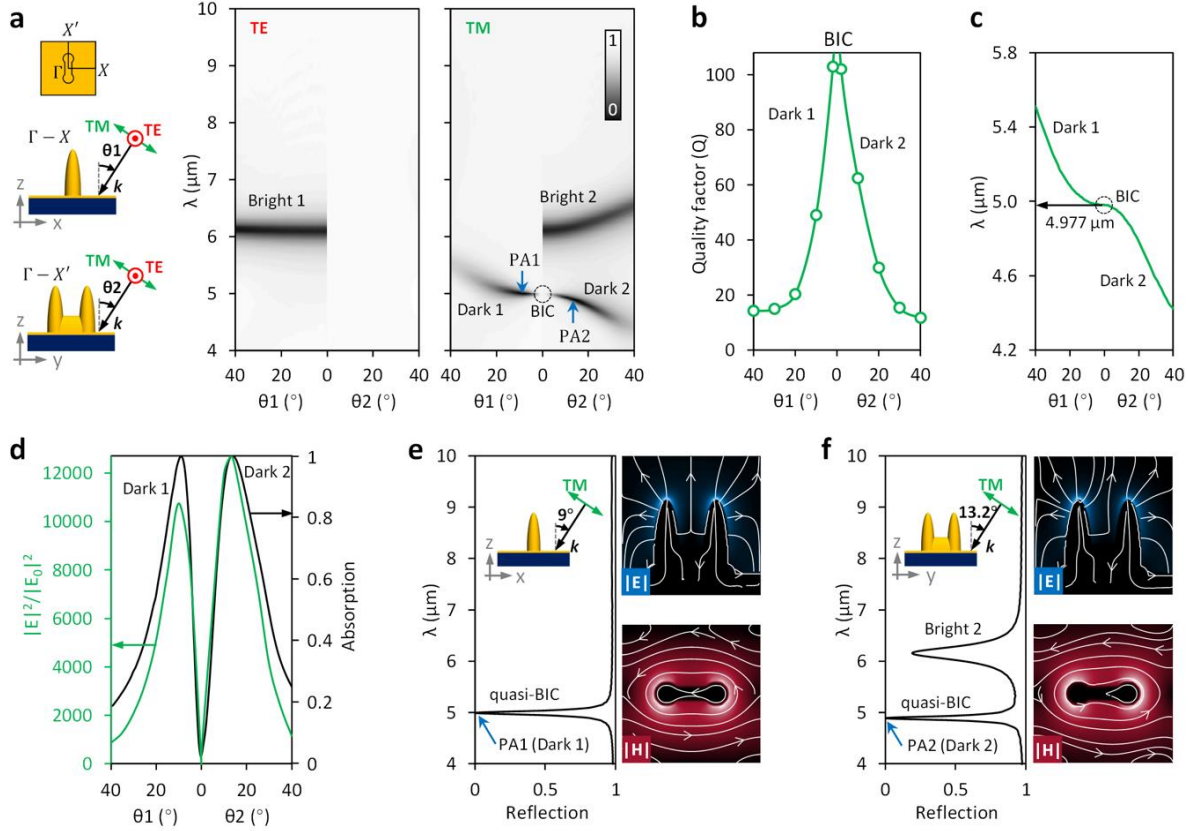

Figure 2. Theoretical results for BICs in plasmonics double-pillar metasurfaces. (a) Simulated reflection spectra for various oblique incidences (band diagrams) for TE- am TM-polarized wves in xz-plane (θ1) and yz-plane (θ2), respectively. BICs are highlighted by dotted circles. The blue arrows point to the regime of perfect absorption (PA) for "Dark 1" and "Dark 2" bands. (b) and (c) Dependence of the quasi-BIC Q factor and wavelength on the angle of incidence along Γ−X (θ1 > 0) and Γ−X' (θ2 > 0) principal axes. (d) Field enhancement and absorption at the quasi-BIC wavelength for different angles of incidence. (e) and (f) The wavelength cut of the simulated reflection map (a) for TM polarization at θ1 = 9° and θ2 = 13.2°, respectively, which correspond to the PA condition at the wavelength of the quasi-BIC, labeled as PA1 and PA2. The insets show the E- and H-field distributions at the resonance wavelengths of the quasi-BIC mode. The instantaneous field directions are represented by the white streamlines.

Figure 2a shows the simulated reflection diagrams along the principal axes of the reciprocal space Γ−X and Γ−X'. For calculations, we use the finite-different time-domain (FDTD) simulations and consider a structure of a finite size with periodic boundary conditions to avoid edge effects (Supporting Information 1). A plasmonic BIC manifests itself as a dark mode at λ = 4.977 μm for the TM polarized excitation, where λ is the resonance wavelength. For the oblique incidence, the BIC transforms into a quasi-BIC with a finite Q_{rad}, which total factor Q_{tot} decreases away from the Γ point (Figure 2b). Here, the Q factor is estimated as $Q_{tot} = \Delta\lambda/\lambda$, where $\Delta\lambda$ is the full width at half-maximum. The quasi-BIC dispersion is strongly anisotropic, and it has opposite sign (red-shift or blue-shift) along Γ−X and Γ−X' bands, which we denote as "Dark 1" and "Dark 2", respectively (Figure 2c). Next, we evaluate the resonant field enhancement at the quasi-BIC wavelength depending on the angle of incidence (Figure 2d). The calculations show that distinct maxima of the field enhancement $|E|^2/|E_0|^2 \sim 10^4$ are achieved for 9° (Γ−X) and 13.2° (Γ−X'), which coincide with the PA condition. Reflection spectra at these specific angles show narrow dips at the quasi-BIC wavelength with Q~50, (Figures 2e,f), for which the absorption is equal to unity. The field profile of the quasi-BIC mode represents an out-of-plane electric dipole (Figures 2e,f and Supporting Information 2). Such a dipolar pattern prohibits radiation out of the surface plane which is consistent with its BIC origin and predicts its robustness to a change of geometrical parameters (Supporting Information 4). The calculated effective mode volume for the quasi-BIC mode at PA1 and PA2 is $V_{eff} \sim 5 \cdot 10^{-4} \lambda^3$, which confirms that the plasmonic metasurface provides deeply subwavelength localization of energy. In simulations, we also observe the mode characterized by an in-plane electric dipolar momentum, which we denote as "Bright" because of its radiative nature (Supporting Information 3, 4).

We use the target design to fabricate the anisotropic plasmonic metasurface and characterize its optical properties. The sample is fabricated by a femtosecond laser via two-photon polymerization, followed by physical vapor deposition of 100-nm layer of gold (Figures 3a,b). Fabrication details are described in Supporting Information 5. Scanning electric microscope (SEM) images of the fabricated sample are shown in Figure 3c.
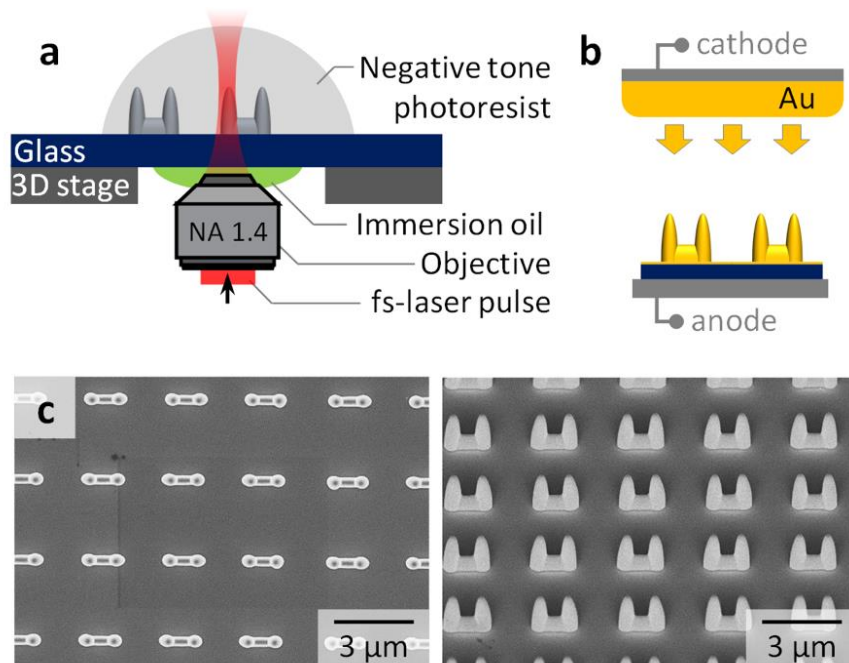

Figure 3. **Fabrication approach**. (a) Fabrication of dielectric double-pillar resonators using the laser writing technique. (b) Metallization of the samples by gold sputtering. The thickness of the gold layer is around 100 nm. (c) The top view and 45° angle view of the nanopillar plasmonic array under the scanning electric microscope (SEM).
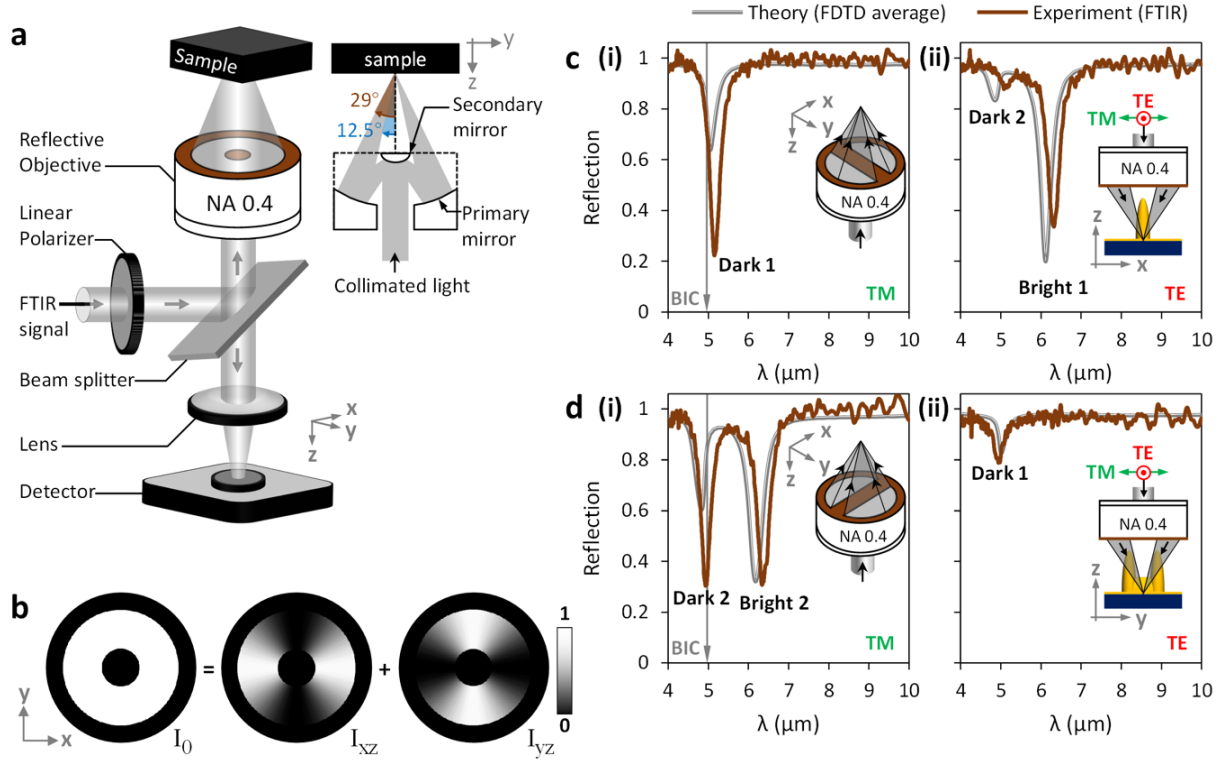
Figure 4. **Experimental demonstration of quasi-BIC modes in anisotropic plasmonic metasurfaces**. (a) Schematic of the FTIR system and reflective objective. (b) The light intensity distribution at the plane of reflective objective and its decomposition into xz- and yz-contributions. (c) and (d) Measured and simulated weighted-average spectra for (i) TM and (ii) TE polarizations. The reflective objective is blocked by a piece of tape along (c) y-axis and (d) x-axis, respectively.

We measure the reflection spectra of the fabricated metasurface by using a FTIR spectrometer (Bruker Vertex 70) equipped with an infrared microscope (Bruker Hyperion 2000). The collimated broadband mid-IR beam passes through a wire-grid polarizer, beam splitter, and then it is focused on the sample by a reflective objective (RO) (Figure 4a). After focusing, the light beam has isotropic angular distribution in the x-y plane and dispersion of polar angles in the range from 12.5° to 29° (Figure 4a and Supporting Information 6). To enable selective excitation of BIC along the principal directions Γ–X and Γ–X' (x- and y-axes, respectively), we block the central part of the

RO in one direction, which partially filters the light coming from the undesired angles. Figure 4b shows the decomposition of light intensity in xz- and yz-planes in the RO. For the unblocked objective, intensity components I_{xz} and I_{yz} are equal (Figure S5d). After applying the opaque tape along one of the axes, the percentage of intensity in the orthogonal plane increases to ~72% while the other intensity component drops to ~28% (Figure S5e). In experiment, we use two orthogonal configurations of the objective blocked with an opaque tape, which helps to improve the selectivity of excitation beyond the limit of the standard FTIR.

Figures 4c,d show experimentally measured reflection spectra for both objective configurations and both polarizations. The spectra clearly show the existence of two dark modes in the TM polarization associated with two different dispersion bands of the quasi-BIC mode. The resonant wavelength of "Dark 1" and "Dark 2" mode is red- and blue-shifted, respectively, in relation to the BIC wavelength, confirming the predicted anisotropy of the quasi-BIC dispersion. We notice that in numerical simulations the PA condition is realized for the angles of incidence around 9-13° (Figures 2e,f) which overlaps with the angular distribution of the pump beam used in experiment. Therefore, in experiment we collect the integral reflected intensity over the resonances in the vicinity of the PA regime, for which the field enhancement is maximal.

We also observe a broader feature in reflected TE and TM signal associated with the bright mode (Figures 4c,d). We notice that the observed Q factors of two quasi-BIC resonances (Q~17) are lower than those predicted in theory (Q~50, see Figures 2e,f), which can be explained by peculiar properties of the FTIR excitation scheme, which uses a beam composed of multiple waves with different angles of incidence. To provide more fair comparison with the experiment, we calculate the simulated weighted-average of the reflected spectra using weight functions of the tape-enhanced objective configurations (Figures 4c,d and Supporting Information 6). The numerical

simulations demonstrate that the angle averaging increases the observed spectral linewidth of the quasi-BIC mode in several times.

The experimentally measured response is in good agreement with the improved simulation predictions. However, that the depth of reflection dip in the experiment is, in general, deeper than that in simulation predictions while the measured resonances have larger linewidth than that predicted. The observed discrepancy is primarily attributed to three reasons. First, the surface roughness together with the spatial and geometrical disorder increase the linewidth in experiment. Second, there are differences in the light collection between simulations and experiments. In the simulation, all the backward scattering light is collected by a monitor. However, in the experiment, the reflective objective only collects partial backward scattering light with a specific angular distribution (Figure S6a). Third, the simulation is based on the assumption of an infinite array, but the finite size of samples in experiments will inevitably introduce deviations in the spectra.

In summary, we have demonstrated, for the first time to our knowledge, how to employ the physics of high-Q resonances associated with bound states in the continuum for lossy metallic metasurfaces by combining it with the extreme field confinement provided by plasmonic structures. We have fabricated and studied experimentally a novel type of anisotropic plasmonic metasurfaces supporting high-Q resonances associated with quasi-BIC collective lattice modes. We have engineered these quasi-BIC modes with highly anisotropic dispersion in the k-space and have identified them through sharp resonances at mid-IR wavelengths. By exciting the quasi-BIC resonances in the vicinity of the perfect absorption regime, we have satisfied the optimal coupling condition, for which the field enhancement becomes the highest. Our results demonstrate a direct and simple way to explore simultaneously the nanostructuring of metallic surfaces to achieve high

Q collective resonances due to the BIC physics combined with a small effective mode volume of plasmonic systems, with many applications requiring strong field enhancement of light-matter interaction such as nonlinear nano-optics, subwavelength lasers, and quantum nanophotonics.

ASSOCIATED CONTENT

Supporting Information

Supporting Information 1: FDTD Simulations; Supporting Information 2: Near-field excitation of dark and bright modes; Supporting Information 3: Far-field excitation of the bright mode; Supporting Information 4: Robustness of high Q quasi-BICs against the change of lattice spacing; Supporting Information 5: Fabrication; Supporting Information 6: Optical characterization.

AUTHOR INFORMATION

Corresponding Authors

E-mail: bjia@swin.edu.au (B.J.) and ysk@internode.on.net (Y.K.).

ORCID

Baohua JIa: 0000-0002-6703-477X

Yuri Kivshar: 0000-0002-3410-812X

Author Contributions

‡These authors (Y.L., K.K. and F.Z.) contributed equally.

Y.L., K.K. and Y.K. developed the conceptual idea. K.K. worked on the theory. F.Z. and K.K. performed FDTD simulations. Y.L., H.L. and B.J. proposed experimental investigations. Y.L. carried out fabrication, SEM, and FTIR measurements. F.Z., H.L., S.L. and J.W. contributed to results interpretation and discussion. K.K., Y.L. and Y.K. designed figures and wrote the manuscript with input from all other authors. B.J., H.L. and Y.K. supervised the research. All authors have given approval to the final version of the manuscript.

Notes

The authors declare no competing financial interest.

REFERENCES

1. Maier SA. Plasmonics: fundamentals and applications. Springer; 2007.

2. Schuller JA, Barnard ES, Cai W, Jun YC, White JS, Brongersma ML. Plasmonics for extreme light concentration and manipulation. *Nature Materials* 2010; 9(3):193-204.

3. Zhou W, Dridi M, Suh JY, Kim CH, Co DT, Wasielewski MR, et al. Lasing action in strongly coupled plasmonic nanocavity arrays. *Nature Nanotechnology* 2013; 8(7):506-511.

4. Yang A, Hoang TB, Dridi M, Deeb C, Mikkelsen MH, Schatz GC, et al. Real-time tunable lasing from plasmonic nanocavity arrays. *Nature Communications* 2015; 6(1), *6939.*

5. Wang W, Ramezani M, Väkeväinen AI, Törmä P, Rivas JG, Odom TW. The rich photonic world of plasmonic nanoparticle arrays. *Materials Today* 2018; 21(3):303-314.

6. Kuznetsov AI, Miroshnichenko AE, Brongersma ML, Kivshar YS, Luk'yanchuk B. Optically resonant dielectric nanostructures. *Science* 2016; 354(6314): aag2472.

7. Kruk S, Kivshar Y. Functional meta-optics and nanophotonics governed by Mie resonances. *ACS Photonics* 2017; 4(11):2638-2649.

8. Auguié B, Barnes WL. Collective resonances in gold nanoparticle arrays. *Physical Review Letters* 2008; 101(14):143902.

9. Reshef O, Saad-Bin-Alam M, Huttunen MJ, Carlow G, Sullivan BT, Ménard J-M, et al. Multiresonant High-Q Plasmonic Metasurfaces. *Nano letters* 2019; 19(9):6429-6434.

10. Neubrech F, Huck C, Weber K, Pucci A, Giessen H. Surface-enhanced infrared spectroscopy using resonant nanoantennas. *Chemical Reviews* 2017; 117(7):5110-5145.

11. Hsu CW, Zhen B, Stone AD, Joannopoulos JD, Soljačić M. Bound states in the continuum. *Nature Reviews Materials* 2016; 1(9):16048.

12. Hsu CW, Zhen B, Lee J, Chua S-L, Johnson SG, Joannopoulos JD, et al. Observation of trapped light within the radiation continuum. *Nature* 2013; 499(7457):188-191.

13. Jin J, Yin X, Ni L, Soljačić M, Zhen B, Peng C. Topologically enabled ultrahigh-Q guided resonances robust to out-of-plane scattering. *Nature* 2019; 574(7779):501-504.

14. Bulgakov EN, Maksimov DN. Topological bound states in the continuum in arrays of dielectric spheres. *Physical Review Letters* 2017; 118(26):267401.

15. Koshelev K, Favraud G, Bogdanov A, Kivshar Y, Fratalocchi A. Nonradiating photonics with resonant dielectric nanostructures. *Nanophotonics* 2019; 8(5):725-745.

16. Rybin MV, Koshelev KL, Sadrieva ZF, Samusev KB, Bogdanov AA, Limonov MF, et al. High-Q supercavity modes in subwavelength dielectric resonators. *Physical Review Letters* 2017; 119(24):243901.

17. Koshelev K, Lepeshov S, Liu M, Bogdanov A, Kivshar Y. Asymmetric metasurfaces with high-Q resonances governed by bound states in the continuum. *Physical Review Letters* 2018; 121(19):193903.

18. Kodigala A, Lepetit T, Gu Q, Bahari B, Fainman Y, Kante B. Lasing action from photonic bound states in continuum. *Nature* 2017; 541(7636):196-199.

19. Ha ST, Fu YH, Emani NK, Pan Z, Bakker RM, Paniagua-Dominguez R, et al. Directional lasing in resonant semiconductor nanoantenna arrays. *Nature Nanotechnology* 2018; 13(11):1042-1047.

20. Yesilkoy F, Arvelo ER, Jahani Y, Liu M, Tittl A, Cevher V, et al. Ultrasensitive hyperspectral imaging and biodetection enabled by dielectric metasurfaces. *Nature Photonics* 2019; 13(6):390-396.

21. Koshelev K, Kruk S, Melik-Gaykazyan E, Choi J-H, Bogdanov A, Park H-G, et al. Subwavelength dielectric resonators for nonlinear nanophotonics. *Science* 2020; 367(6475):288-292.

22. Cong L, Singh R. Symmetry‐Protected Dual Bound States in the Continuum in Metamaterials. *Advanced Optical Materials* **2019**, *7*, (3), 1900383

23. Abujetas DR, van Hoof N, ter Huurne S, Gómez Rivas J, Sánchez-Gil JA. Spectral and temporal evidence of robust photonic bound states in the continuum on terahertz metasurfaces. *Optica* **2019,** *6, (8) 996-1001.*

24. Azzam SI, Shalaev VM, Boltasseva A, Kildishev AV. Formation of bound states in the continuum in hybrid plasmonic-photonic systems. *Physical Review Letters* 2018; 121(25):253901.

25. Xiong X, Jiang SC, Hu YH, Peng RW, Wang M. Structured metal film as a perfect absorber. *Advanced Materials* 2013; 25(29):3994-4000.

26. Zhou W, Odom TW. Tunable subradiant lattice plasmons by out-of-plane dipolar interactions. *Nature Nanotechnology* 2011; 6(7):423-427.

27. Maier SA. Plasmonic field enhancement and SERS in the effective mode volume picture. *Optics Express* 2006; 14(5):1957-1964.

28. Yariv A. Critical coupling and its control in optical waveguide-ring resonator systems. *IEEE Photonics Technology Letters* 2002; 14(4):483-485.

29. Bliokh KY, Bliokh YP, Freilikher V, Savel'ev S, Nori F. Colloquium: Unusual resonators: Plasmonics, metamaterials, and random media. *Reviews of Modern Physics* 2008; 80(4):1201.

30. Gorodetsky ML, Ilchenko VS. Optical microsphere resonators: optimal coupling to high-Q whispering-gallery modes. *JOSA B* 1999; 16(1):147-154.
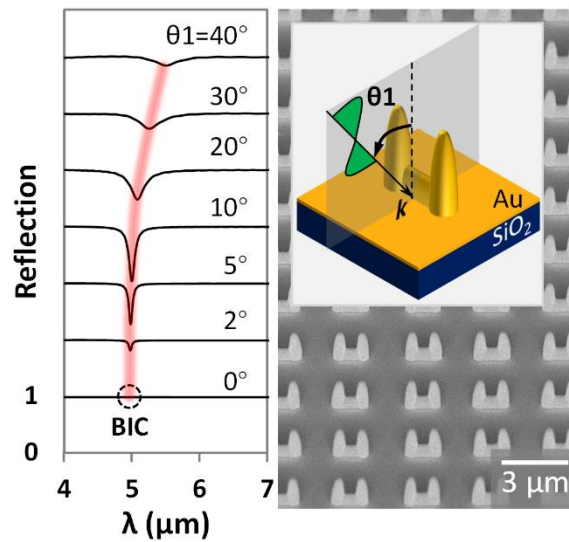
TOC image

Table of Contents (TOC) graphic. Left: Reflection spectra of the plasmonic metasurface for various angles of incidence. Evolution of the quasi-BIC resonance with respect to the angle variation is highlighted. Right: Schematic of the unit cell and the SEM image of the fabricated metasurface.